MOLECULAR MODELING AND 3D ANALYSIS OF WATER STRESS RESPONSIVE *TAPASE* PHOSPHATASE ENCODING GENE IN WHEAT (*TRITICUM AESTIVUM*)

ARUN DEV SHARMA

Department of Biotechnology, Lyallpur Khalsa College, G T Road, Jallandhar-144001, Punjab, India, Ph-+91-181-2241466, Fax:+91-181-2241465; arundevsharma47@gmail.com

Abstract. Acid phosphatases are key enzymes involved inorganic phosphorous acquisition under stress conditions thus implicated in crop productivity. The present study was designed to perform molecular modeling and 3D analysis of stress responsive acid phosphatase gene TaPase. It has been observed that TaPase encodes protein which is soluble in nature. Based upon these results, a possible physiological role of TaPase in wheat was discussed. It was predicted that TaPase protein is disordered at N-terminal, posses signal peptide, rich in random coils, basic in nature and having polar amino acids. In addition, TaPase protein was modeled using QUARK server followed by validation using VADAR and QMEAN servers which revealed good nature of 3D structure. Functional analysis using PROFUNC server revealed potential role of TaPase under stress conditions along with hydrolytic activity. PDB sum motif analysis revealed Beta–Turns rich profiles in TaPase protein. Based on these findings the possible role of TaPase gene was discussed

Keywords: Abiotic stresses, phosphatases, *TaPase*, 3D Modelling, wheat

Abbreviations:
TaPase: *Triticum aestivum* acid phosphatase
ORF: open reading frame
SP: signal peptide
Pi: inorganic Phosphate
CC: Cellular component category
BP: Biological process category
BF: biological function category

INTRODUCTION

Acid phosphatase (APases) are widespread in nature and undoubtedly implicated in acquisition of phosphates reserves and Pi containing derivatives (inorganic phosphorous: Pi) from soils (Wang et al., 2014; Lin et al., 2009). Acid phosphatases (APase) are a type of Multigene phosphatases and contains a binuclear metal ion center, which hydrolyses a wide range of phosphate esters and anhydrides under optimal acidic conditions. APase's have conserved motifs (DXG/GDXXY/GNH(D/E)/VXXH/GHXH, bold letters represent invariant residues), which can coordinate the binuclear metal center to hydrolyse Pi (Wang et al., 2014). Additionally, several of them have been studied and demonstrated to participate in Pi utilization and mobilization (Song et al., 2014). Multigene families of plant APase's have been reported in *Arabidopsis* (Hurley et al., 2010), rice (Zhang et al., 2011), soybean (Li et al., 2017) and maize (Gonzalez-Munoz et al., 2015).

Mostly, in soils, organic phosphorous comprises 30-80%, however largest fraction (about 50%) exit in the form of phytin derivatives. Plant use "Pi" from soils after hydrolyzing "Pi" sources with acid phosphatases. Under acidic conditions,

APases have shared ability to catalyse the hydrolysis of orthophosphate monoesters. "Pi" have been reported to play very important role in various biological processes: respiration, photosynthesis, metabolic regulation, energy transfer under normal and stress conditions (Tang et al 2017; Kong et al . 2018). The activity of APase is influenced by number of developmental factors like seed, embryo, roots, shoots and environmental factors like soil Pi status, pH of rhizopshere (Tian et al., 2012; Lu et al., 2016). However, it is generally believed that enhanced activity of APase can be beneficial to stressed plants. In addition to Pi scavenger activity , APase have been implicated also in seed dormancy, cell was regeneration, embryo germination (Olzzak and Watorek 2003). Earlier, cloning and expression analysis of stress responsive gene *TaPase* was reported from wheat (Sharma 2010). In this study, in order to gain insight into the biological role of acid phosphatase (*TaPase*) from wheat, molecular modeling and *in-silico* analysis was performed. Further, the non-availability of 3-D structure of *TaPase* encouraged us to predict its 3-D structure and organization using molecular modelling. Using *in-silico* approach, the structural investigation of *TaPase* conducted by studying its tertiary structure, biochemical properties, and identifying the catalytic active sites to achieve a superior contemplative vision of the role of *TaPase* sequence-structure-function association. The structure and function portrayal of *TaPase* will lay a sturdy underpinning to gain an understanding into its imperative function during water stress and also to engender new ideas to expound their function. During the past, *In-silico* approaches have contributed massively to untangle stress responses. The dusk of new technologies, principally after the 'post-genomic' era, authorized foresights into the intricacy of plant responses (Oono et al. 2003). Hence, numerous water stress responsive genes can be annotated *in-silico*, and expectantly they can provide voracious information for considerate the mechanisms of the abiotic stress tolerance. Consequently, bearing in mind the importance of *in-silico* analysis, in the present study, 3D modeling of water stress responsive gene *TaPase* from wheat was investigated.

MATERIAL AND METHODS

Plant material and DNA isolation

The wheat seeds were surface sterilized with 1% (w/v) mercuric chloride followed by 70 % (v/v) ethanol. Seeds were thoroughly rinsed with deionized water and imbibed for 6 h. After imbibition, seeds were placed in Petri plates containing sterile filter sheets, moistened with water. The plates were incubated at 37 ±1°C in a seed germinator in darkness and allowed to grow for 5 days. The shoots were harvested and used for DNA isolation. DNA was isolated from the pooled shoots following CTAB method as per Sharma et al. (2002).

Sequence analysis of TaPase

The *TaPase* was amplified using specific primers from *Lupinus luteus* acid phosphatase gene (AJ458943) using forward 5'-CAAGGATGCGGGTTGTGTTGC-3' and reverse 5'- CATGCTCACAGCTTCATCAACAAG-3' primers . The reaction was carried out as per following conditions: initial denaturation 5 min, followed by 35 cycles of denaturation (94°C, 30 sec), annealing (55°C, 30 sec), and extension (72°C, 3 min) and final incubation (72°C, 10 min). The PCR product was run on 2% agarose gel

and the desired band of about 500 bp was excised, eluted and purified as per manufacturer's protocol (Genei). The PCR product was cloned into TA vector and sequenced (pGEMT®-Easy) (Fig. 1).The sequence data has been deposited at Genbank under accession no EU 723832. Subsequently , the gene sequence was retrieved and subjected to ORF analysis. Sub-Cellular localization analysis was made by using Target P (http://www.cbs.dtu.dk/services/TargetP/) and Phobius online tools (http://phobius.sbc.su.se/). Signal P 4.1 was used to find out any signal sequence peptide ((http://www.cbs.dtu.dk/services/SignalP-4.0/). Disorder nature of *TaBsSRP3* was determined by PONDER fit online tool (http://www.pondr.com/). Conserved regions were isolated by using CLUSTAL-W analysis (http://www.genome.jp/tools-bin/clustalw). Phylogenetic tree was constructed using NJ method by MEGA 4 tool. MINNOUS server (POLYVIEW 2D tool) was used to determine transmembrane domain (http://polyview.cchmc.org/). Hydropathy analysis was carried out by using ProtScale tool at ExPASy (https://web.expasy.org/protscale/). Secondary structure predication was conducted by using PSIPRED (http://bioinf.cs.ucl.ac.uk/psipred/) and GOR 3 tool (https://npsa-prabi.ibcp.fr/cgi-bin/npsa_automat.pl?page=/NPSA/npsa_gor4.html). Hydrophobic cluster analysis as carried out using Mobyle tool (http://mobyle.rpbs.univ-paris-diderot.fr/cgi-bin/portal.py?form=HCA#forms). Protparam tool (https://web.expasy.org/protparam/) was used to find out isoelectric point (PI), various physicochemical properties, composition of the amino acids, instability index, molecular weight and GRAVY Score. Predicting the geometry of metal binding sites from protein sequence was detected using Metal Detector prediction tool (http://metaldetector.dsi.unifi.it/v2.0/).

3-D Modeling (3-D) and evaluation of TaPase protein

For modeling TaPase protein sequence was submitted to QUARK online server for 3 D modeling (https://zhanglab.ccmb.med.umich.edu/QUARK2/output/QA7681/). Structural validation was carried out using VADAR (http://redpoll.pharmacy.ualberta.ca/vadar) and QMEAN (https://swissmodel.expasy.org/qmean/) tools. To analyze structural motifs, PDB file of modelled TaPase protein was submitted to PDBsum (www.ebi.ac.uk/pdbsum/). Biochemical function of TaPase was studied using ProFunc server of EMBL-EBI (http://www.ebi.ac.uk/thornton-srv/databases/ProFunc. ProFunc server of EMBL-EBI was used to find out the biochemical role of TaPase based upon its structure. Ligand binding sites were calculated by using COFACTOR tool (https://zhanglab.ccmb.med.umich.edu/COFACTOR/).

Catalytic active site prediction

In order to find out active site regions on 3-D structure of TaPase, CASTp tool was used (http://sts.bioe.uic.edu/castp/index.html?3trg).

RESULTS AND DISCUSSION

A 516 bp DNA designated as *TaPase* (*Triticum aestivum* acid phosphatase) was amplified and cloned into TA vector (pGEMT®-Easy) and submitted to GenBnak database (accession no Eu732823). Further, 3-D modeling and analysis of *TaPase* using *in-silico* approaches has been performed. For this, *TaPase* gene sequence was retrieved from GenBnak database and subjected to open reading frames (ORFs) analysis. Interestingly, only two ORFs from *TaPase* gene have been retrieved on negative frames. One longest ORF consisting 44 amino acids were retrieved and selected for further studies.

Interestingly, Clustal-W analysis of 13 plant acid phosphatases gene sequences revealed the presence of conserved regions in *TaPase* along with all the reported gene sequences (fig. 1A), indicating that tryptophan residue may be involved in catalytic activity of *TaPase* encoding proteins. Earlier reports also indicated that tryptophan's are found as part of the phosphate binding sites in a number of phosphatase proteins in plants and animals (Rao et al., 1996). Multiple amino acid sequence analysis using various phosphatase proteins from various species (Fig. 1B), indicated characteristic conserved consensus sequence, designated as "LLALALVLNVVVVSNGGKSSNFVRKT-N-----KNRDMPLDSDVFRVP".

Phylogenetic studies of TaPase, clearly indicated the existence of 3 major clades, indicating a divergent and independent evolution of acid phosphatases in different plant species (fig. 1C). Metal-Detector tool identified HIS 32 residue, which is reported to be involved in transition metal protein binding sites. Metallo-proteins are a large and diverse class of proteins which bind one or more metal ions in their native conformation and play a wide range of structural, regulatory or catalytic roles which are critical to protein function (Degtyarenko et al., 2000). Antonyuk et al (2014) also reported the role of HIS residue of PPD1 acid phosphatase in metal binding from yellow lupin seeds.

MINNOUS server (POLYVIEW 2D tool) analysis also showed that TaPase protein is soluble in nature and devoid of any transmembrane domain (TM domain). Using PONDR-fit prediction tool revealed that C- terminal of TaPase was disordered with intrinsic disordered score of 0.51, constituting 59 % overall percent disordered with C terminal residues, demonstrating extremely disordered character of the protein (fig. 2A). Intrinsic disordered regions are important in the function of many proteins (Fox et al., 2017). Due to dynamic flexible in nature, disordered proteins assumes various conformational changes for binding enzymes and receptors implicated in cell signalling and transcription functions (Fox et al., 2017). Hydropathy plot analysis also revealed that, most amino acid residues (towards C terminal) scored near to 0-0.5 score (fig. 2B), indicating hydrophilic nature of most residues. These findings indicated that amino acid residues of TaPase are likely to stay in touch with solvent or water, and therefore, they tend to reside on outer surface of the protein. The secondary structure prediction by GOR4 tool, I-TASSER and PSIPRED tools predicts that ~ 84% of TaPase is in random coil conformation and rest of the sequence is predicted to assume extended strand conformation (fig. 2C). Notably, just 3 amino acids (Leu:30,Asn:N31,His:32) were involved in helix conformation. Due to this feature, protein structure assumes flexibility under water stress enabling it to bend, stretch and

enlarge in all the probable orders to fasten water molecules thus defending bio membranes from dehydration. Signal P server predicted that TaPase has a 24 amino acid signal peptide (SP) at its N-terminus, indicating secretary nature of the protein (fig 3A). The predicted cleavage site was alanine "Ala 23". Monod et al (1989) mentioned that processing and secretion of acid phosphatases is always normal when amino acid at cleavage position is any neutral amino acid like: alanine, glycine, cysteine, serine or threonine. Phobius tool further validated TaPase protein as non cytoplasmic and indicated signal peptide from 1-24 amino acids towards N-terminal part of TaPase (fig 3B). A signal peptide (SP), also called as targeting signal/transit peptide is a short stretch of amino acid stretch mostly situated at N-terminus of majority of newly synthesized proteins, which reside inside organelles or targeted towards secretary pathway. Based on these findings, it was postulated that under stress conditions delivery of phosphate (Pi) is impaired thus resulted in activation of *TaPase* gene. Consequently, by virtue of having SP, TaPase released outside of the cells thereby modulate osmotic adjustment by free phosphate uptake mechanism.

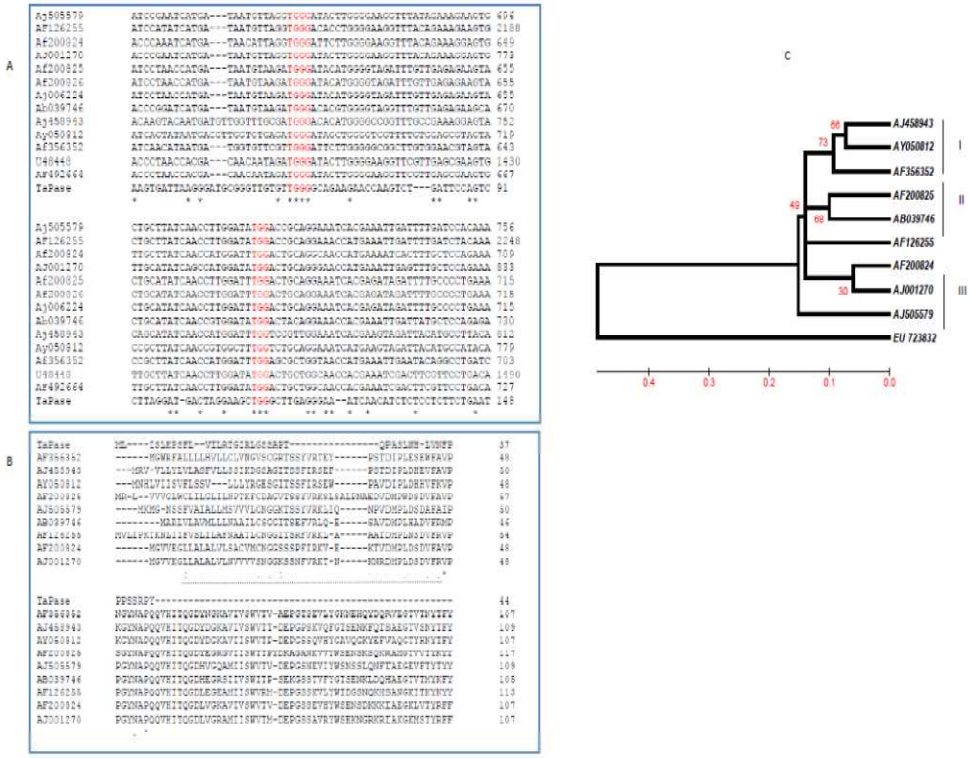

Fig. 1. Clustal-W analysis of TaPase with different reported phosphatases genes (A), amino acids (B) and phylogenetic analysis (C). Aj505579:*Lupinus luteus*, AF126255:*Anchusa officilanus*; Af200824: *Glycine max*; AJ001270:*Phaesolus vulgaris*; Af200825: *Ipomoea batatas*; Af200826; *Ipomoea batatas*; Aj006224: *Ipomoea batatas*; Ab039746:*Spirodela oligrrhiza*; Aj458943: *Lupinus luteus*; Ay050812: *Arabidopsis thaliana*; Af356352; *Oriza sativa*; U48448: *Arabidopsis thaliana*; AF492664: *Arabidopsis thaliana*; TaPase: present study EU723832.* indicate conserved residues. Dotted line indicate conserved consensus motif

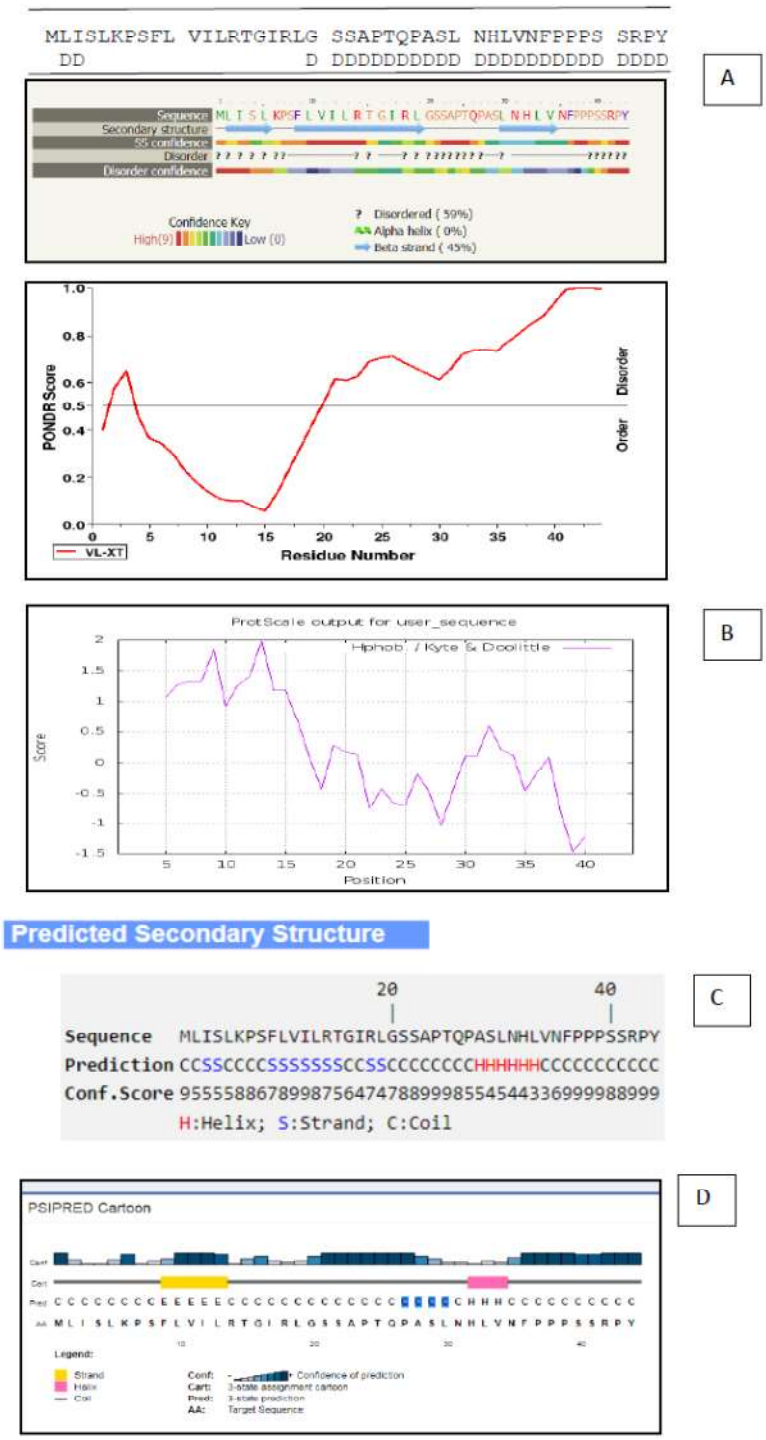

Fig. 2. PONDER fit (A), Hydropathy analysis (B) and PSIPRED (C and D), analysis of TaPase protein.

Further, hydrophobic cluster analysis using Moyble tool revealed that SP contained a long stretch of hydrophobic amino acids (FLVIL) that have tendency to form alpha –helix and also termed as "h-region" (Fig.3C). I-TASSER server also predicted the solvent accessibility score of "h-region" residues from 0-2, indicating buried nature of these residues. Cellular localization predicted by Target P online tool validated TaPase to be a mitochondrial protein. Earlier studies based immune-localization data also recognized that phosphatases are mainly localized in mitochondria and plastids (Liao et al., 2003). B- factor profile (BFP) analysis as defined by the degree of inherent thermal mobility of residues/atoms in proteins for widely held of residues was nearly zero (fig. 3D).

Using Protparam tool, the isoelectric point and molecular weight of TaPase was found to be 11.72 and 4.7 kDa, respectively (Table 1). Besides, the sequence has a high and negative electrical charge [negatively charged: Asp + Glu: 0; positively charged: Arg + Lys: 4 residues]. This difference explains the highly basic nature of the protein and high pI. The Aliphatic index of TaPase as measured by the relative volume occupied by aliphatic amino acids (alanine, valine, isoleucine, and leucine) was 106.36 indicating that TaPase may be thermostable in nature. Moreover, upon sequence analysis, it was observed that TaPase posses high content of proline (15.9%), serine (15.9%), leucine (15.9%). Proline residues due to cyclic structure ideally suited for beta turns and play fundamental and subtle role in protein function, protein structure and protein- protein interaction (Marcelino and Gierasch, 2008). Proline residue has been implicated in providing rigidity to protein chain by imposing certain torsion angles on the segment of the structure. Due to high content of serine, it may possible that TaPase may be involved in protein stability, kinase domain function, or modulates a protein binding interaction. "N-end rule", by PROTPARAM tool, indicated that the TaPase was quite stable as indicated by estimated half life [30 hours (mammalian reticulocytes, in vitro); >20 hours (yeast, in vivo); >10 hours (*Escherichia coli*, in vivo)]. Hydropathy plot and GRAVY score (0.186) of TaPase (Fig. 2B, Table 1) also indicated it to be likely hydrophilic nature of TaPase. Moreover, upon sequence analysis, it was observed that TaPase posses hydrophilic (Arg: 6.8%), highly polar and charged residues (Ser: 15.9%; Thr: 4.5%; Asn: 4.5% and Tyr: 2.3%), and amphipathic tryptophan (2.3%). The massive sum of polar and hydrophilic residues in TaPase provides a flexible backbone which account for their high potential and characteristic features as thermostable proteins. The TaPase protein may be an extremely extensional distinction because of the abundance of the polar amino acids.

In protein research in order to find out structure-function relationship and biological function analysis, prediction of 3 D structure is apt to study protein function, protein-protein interaction, ligand interaction and enzyme catalysis. Five structure models for TaPase were predicted by QUARK, which is based on algorithm for *ab-initio* protein structure prediction and protein peptide folding, and the best model is shown in Fig.4A. The identified model had depicted three sandwiched β-sheets at N-terminal and one helix region at C-terminal (fig. 4). Olczak et al (2003) also reported that kidney red bean acid phosphatase also formed N- terminal domain by forming two β sandwiched sheets, each composed of three β antiparallel strands. In another study, acid phospahatase PPD1 from yellow lupin seeds, two β sandwiched sheets at N-terminal also have been detected (Antonyuk et al., 2014). Swiss-Pdb Viewer tool was

used for energy minimization of the predicted model for the stabilization of their stereo-chemical properties. Swiss-Pdb Viewer tool was used for energy minimization of the predicted model for the stabilization of their stereo-chemical properties. Structural validations and quality assessment as carried out by using VADAR (Fig. 4B). VADAR server that included parameters like 3D quality index and stereo packaging quality index were found to be good (fig 4C). QMEAN server also confirmed the model as good, (fig. 4D).

Ligand binding sites of TaPase protein were also predicted by COFACTOR tool and the most excellent ligand binding site is shown in the fig. 5A. Predicted ligand was a "CTP", (CYTIDINE TRIPHOSPHATE) (analogue to ATP). CTP is a coenzyme involved in many metabolic reactions like the synthesis of glycerophospholipids and glycosylation of proteins. All acid phosphatases are N-glycosylated which is typical feature of secreted enzymes (Olczak et., 2003). The predicted binding site residues were L13, T 15, I17 (Fig 5A), indicating key involvement of TaPase in metabolic processes. Biological function of TaPase 3D model was predicted by ProFunc server which revealed various gene ontology (GO) terms like mitochondrion region in CC (Cellular component) category; response to stimuli in BP (Biological process) category; and catalytic or hydrolase activity in BF (biological function) category.

Structural Motif scan investigation using PDB server showed the incidence 2 different types of beta turns in TaPase protein. Turn from Gln26-Ser29 (QPAS) belonged to type 1 and turn from Leu30-Leu33 (LNHL) was type IV. Being smallest secondary structure, β-turns constitutes about 25% of the residues in proteins. It was observed that motif LNHL from β-turn IV was also involved in formation of helix (fig 5B). *In-silico* detection of active sites in the protein structure has increasingly become area of interest by virtue of having involvement in ligand bindings and enzyme catalysis. Usually ligand binding sites present in the largest interacting cavity having major binding surface.

The binding clefts/cavities were analyzed by CASTp prediction tool. Notably, one largest pocket having residues "RLGSSAPQLVN" with area 1.896 and volume 0.85 was detected in CASTp analysis (Fig 5C). Earlier studies also reported that the active site comprises a characteristic set of highly conserved amino-acid residues binding to the dinuclear metal centre. Divalent metal coordinates an asparagine (N) and a terminal aqua ligand (Antonyuk et al., 2014). Notably, proline (P) was also detected in this largest pocket. Antonyuk et al (2014), also postulated that proline is active residue of N-terminal PAP domain found in many acid phosphatases, may be involved in substrate specificity. In addition, few active site residues from cavity were also fashioned part of the structure motifs β-turns. For instance, active site residues Gly 26 and Leu 31 from major cavity 1 formed a part of beta turn, suggestive that it may be key pocket in active site and or participate in enzyme catalysis. Based on these findings it can be postulated that besides being part of active clefts, these residues may be involved in the formation of structural motifs having phosphatase activity.

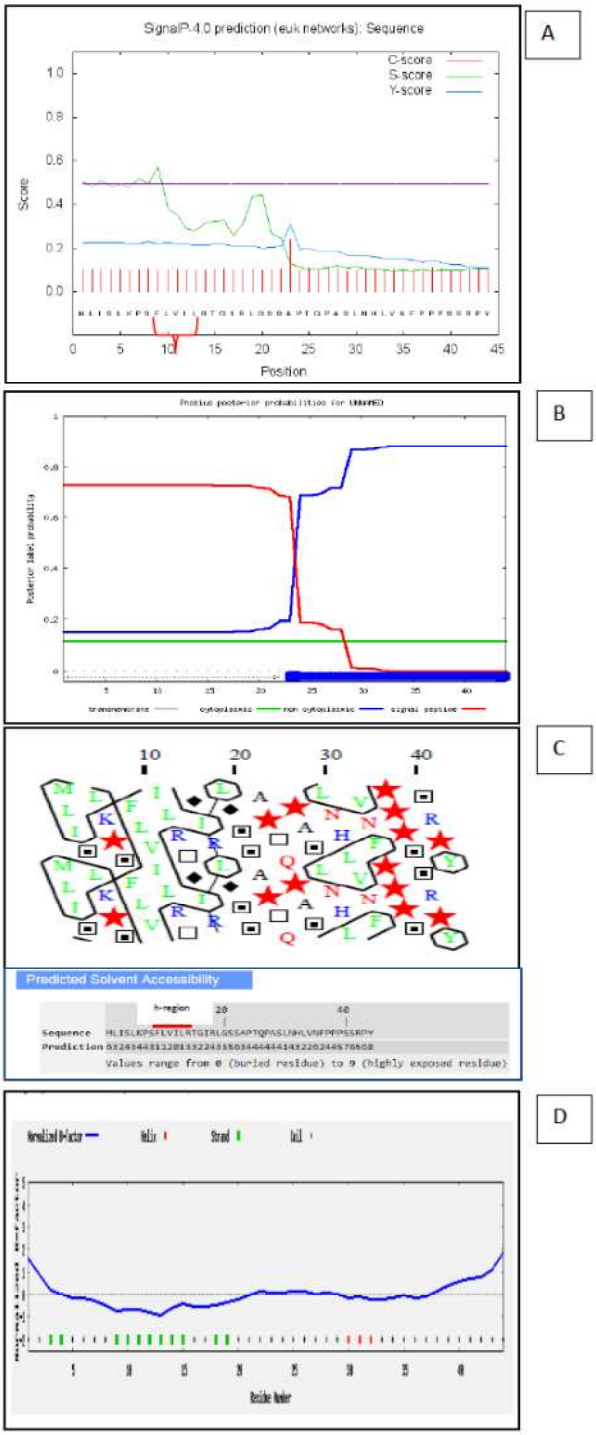

Fig. 3. Signal P (A), cellular prediction by Phobius tool (B), hydropathical cluster analysis by Mobyle tool (C) and predicted normalized B- Factor (D) of TaPase protein sequence

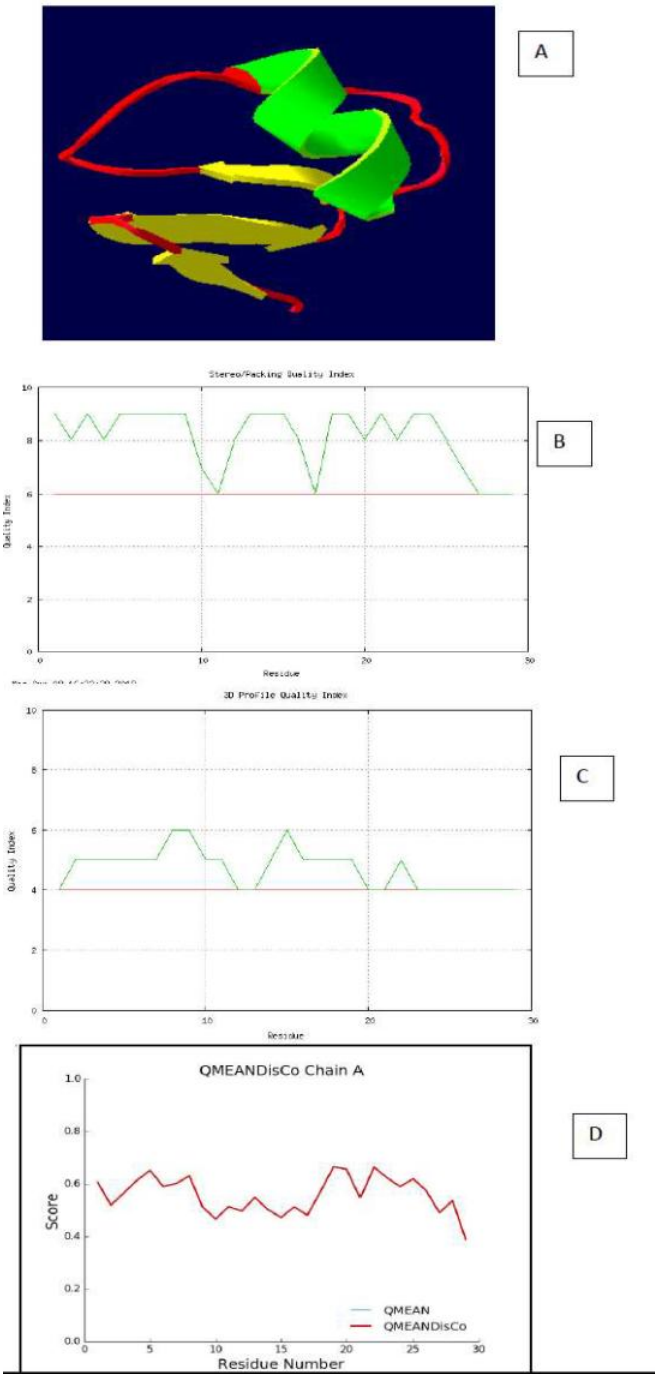

Fig. 4. 3D structure of TaPase. Coils: red; Sheets: Yellow; helix: green (color figure online) (A). VADAR (B, C), and QMEAN (D) analysis of TaPase 3D structure

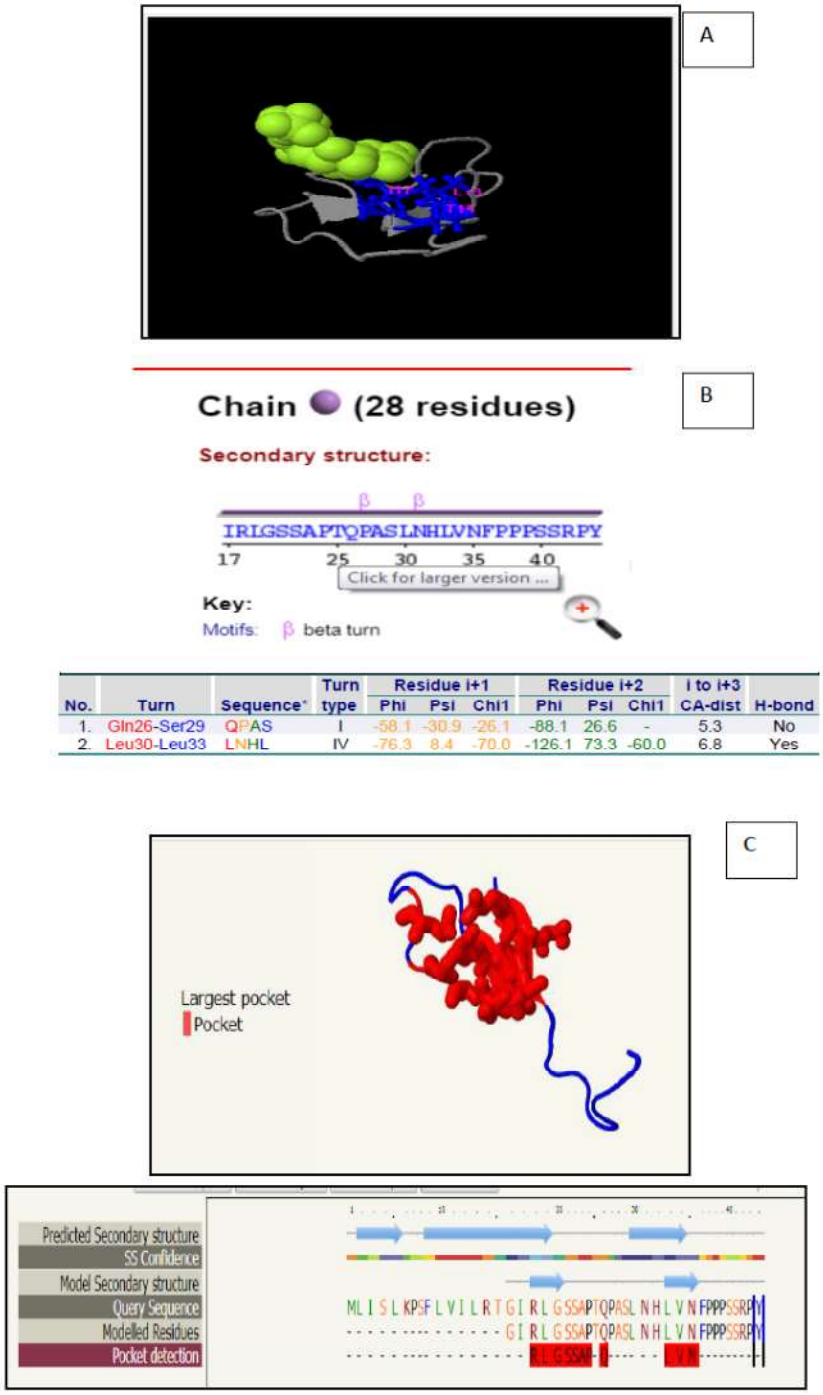

No.	Turn	Sequence*	Turn type	Residue i+1 Phi	Psi	Chi1	Residue i+2 Phi	Psi	Chi1	i to i+3 CA-dist	H-bond
1.	Gln26-Ser29	QPAS	I	-58.1	-30.9	-26.1	-88.1	26.6	-	5.3	No
2.	Leu30-Leu33	LNHL	IV	-76.3	8.4	-70.0	-126.1	73.3	-60.0	6.8	Yes

Fig. 5. Ligand binding site analysis (A). Structural motif analysis of TaPase generated by PDBsum server (Color figure online) (B). CASTp binder site analysis of cavities in TaPase (C)

Table 1

Physiochemical properties of *TaPase*

Parameter	Specification
Molecular weight	4774.65 (Da)
Theoretical pI	11.72
Pro (P) 7	15.9%
Ser (S) 7	15.9%
Leu (L) 7	15.9%
Ile (I) 3	6.8%
Ala (A) 2	4.5%
Arg (R) 3	6.8%
Asn (N) 2	4.5%
Thr (T) 2	4.5%
Tyr (Y) 1	2.3%
Val (V) 2	4.5%
Total number of negatively charged residues (Asp + Glu)	0
Total number of positively charged residues (Arg + Lys)	4
Formula:	$C_{219}H_{355}N_{59}O_{58}S_1$
Total number of atoms	692
Ext. coefficient	1490
The estimated half-life is:	30 hours (mammalian reticulocytes, in vitro). 20 hours (yeast, in vivo). 10 hours (Escherichia coli, in vivo).
Aliphatic index	106.36
Grand average of hydropathicity (GRAVY)	0.186

CONCLUSIONS

The present study was based on 3D analysis and modeling of TaPase protein. The modeled protein structure was rich in stability oriented residues like proline and motifs like beta turns. In addition, it was observed that TaPase protein is intrinsically disordered in nature having signal peptide sequence at N-terminus indicating its secretary nature. Based on the ProFunc, PDB Sum and CAST-P analysis, it was observed that 3-D structural investigation of TaPase also delivers the same point as is inward from previous expression study (Sharma 2010), indicating its possible role in stress adaptation.

ACKNOWLEDGEMENT. AD Sharma would like to thank DST, Govt. of India and Madam Balbir Kaur, President LKC for providing financial assistance for the present study.

REFERENCES

1. Antonyuk, S.V., Mariusz Olczak, A., Olczak, T., Ciuraszkiewiczb, J., Strange, R.W. (2014). The structure of a purple acid phosphatase involved in plant growth and pathogen defence exhibits a novel immunoglobulin-like fold, IUCr J, vol. 1, 101–109.

2. Fox S.,J, Kannan S. (2017). Probing the dynamics of disorder, Progress in Biophy. Mol Biol., vol . 128: 57–62.

3. Gonzalez-Munoz, E., Avendano-Vazquez, A. O., Montes, R. A., de Folter, S., Andres-Hernandez, L., Abreu-Goodger, C., et al. (2015). The maize (Zea mays ssp. mays var.

B73) genome encodes 33 members of the purple acid phosphatase family, Front. Plant Sci., vol. 6, 41

4. Hurley, B. A., Tran, H. T., Marty, N. J., Park, J., Snedden, W. A., Mullen, R. T., et al. (2010). The dual-targeted purple acid phosphatase isozyme AtPAP26 is essential for efficient acclimation of Arabidopsis to nutritional phosphate deprivation, Plant Physiol., vol. 153, 1112–1122.

5. Kong, Li, X., Wang, B., Li, W., Du, H., Zhang C (2018) The Soybean Purple Acid Phosphatase GmPAP14 Predominantly Enhances External Phytate Utilization in Plants. Front, Plant Sci., vol 9, 292

6. Liao, H., Wong, F.L., Phang, T.H., Cheung, M.Y., Li, W.Y., Shao, G., Yan, X., Lam, H.M. (2003). GmPAP3, a novel purple acid phosphatase-like gene in soybean induced by NaCl stress but not phosphorus deficiency, Gene, vol. 318, 103–11.

7. Lin, W.Y., Lin, S.I., Chiou, T.J. (2009). Molecular regulators of phosphate homeostasis in plants, J. Expt. Bot., vol . 60, 1427-1438.

8. Li, C., Li, C., Zhang, H., Liao, H., and Wang, X. (2017). The purple acid phosphatase GmPAP21 enhances internal phosphorus utilization and possibly plays a role in symbiosis with rhizobia in soybean, Physiol. Plant., vol . 159, 215–227

9. Lu, L., Qiu, W., Gao, W., Tyerman, S. D., Shou, H., and Wang, C. (2016). OsPAP10c, a novel secreted acid phosphatase in rice, plays an important role in the utilization of external organic phosphorus, Plant Cell Environ., vol . 39, 2247–2259

10. Marcelino A.M., Gierasch L.M. (2008) Roles of beta-turns in protein folding: from peptide models to protein engineering, Biopolymers, vol. 89, 380–391.

11. Monod M., Haguenauer-Tsapis R., Rauseo-Koenig I., Hinnen A. (1989). Functional analysis of the signal-sequence processing site of yeast acid phosphatase, Eur. J. Biochem., vol . 182: 213-21.

12. Olczak M., Morawiecka B.,Watorek W. (2003). Plant purple acid phosphatases-genes, structures and biological function, Acta Biochim. Pol., vol . 50, 1245–1256.

13. Tang, L. P., Zhou, C., Wang, S. S., Yuan, J., Zhang, X. S., and Su, Y. H. (2017). FUSCA3 interacting with LEAFY COTYLEDON2 controls lateral root formation through regulating YUCCA4 gene expression in Arabidopsis thaliana, New Phytol., vol . 213, 1740–1754.

14. Tian, J., Wang, C., Zhang, Q., He, X., Whelan, J., and Shou, H. (2012). Overexpression of OsPAP10a, a root-associated acid phosphatase, increased extracellular organic phosphorus utilization in rice, J. Integr. Plant Biol., vol . 54, 631–639

15. Song, H., Yin, Z., Chao, M., Ning, L., Zhang, D., and Yu, D. (2014). Functional properties and expression quantitative trait loci for phosphate transporter GmPT1 in soybean, Plant Cell Environ., vol . 37, 462–472.

16. Sharma, A.D., Gill, P.K, Singh, P. (2002) DNA Isolation From Dry and Fresh Samples of Polysaccharide-Rich Plants. Plant Mol. Biol. Reporter, vol . 20, 415a-415f.

17. Sharma, A.D. (2010). Expression analysis and Cloning of *TaPase* phosphatase gene in wheat (*Triticum aestivum*), Emirates J. Food Agric, vol . 22, 483-489.

18. Vance, C.P., Uhde-Stone, C., Allan, D.L. (2003). Phosphorus acquisition and use: critical adaptations by plants for securing a nonrenewable resource, New Phytol, vol . 157, 423-447.

19. Wang, L., Lu, S., Zhang, Y., Li, Z., Du, X., and Liu, D. (2014). Comparative genetic analysis of Arabidopsis purple acid phosphatases AtPAP10, AtPAP12, and AtPAP26 provides new insights into their roles in plant adaptation to phosphate deprivation, J. Integr. Plant Biol., vol . 56, 299–314.

20. Zhang, Q., Wang, C., Tian, J., Li, K., and Shou, H. (2011). Identification of rice purple acid phosphatases related to posphate starvation signaling, Plant Biol., vol . 13, 7–15.